

Time-resolved observations of the short period CV SDSS J123813.73-033933.0

S. V. Zharikov¹, G. H. Tovmassian^{1*}, R. Napiwotzki², R. Michel¹, and V. Neustroev^{3,4}

¹ Observatorio Astronómico Nacional SPM, Instituto de Astronomía, UNAM, Ensenada, BC, Mexico
zhar.gag,rmm@astrosen.unam.mx

² Centre for Astrophysics Research, University of Hertfordshire, College Lane, Hatfield AL10 9AB, UK
rn@star.herts.ac.uk

³ Computational Astrophysics Laboratory, National University of Ireland, Galway, Newcastle Rd., Galway, Ireland
benj@it.nuigalway.ie

⁴ Isaac Newton Institute of Chile, Kazan Branch

Received — 9 June 2005, accepted — 11 October 2005

ABSTRACT

Aims. We observed a new and poorly studied cataclysmic variable (CV) SDSS J123813.73-033933.0 to determine its classification and binary parameters.

Methods. Simultaneous time-resolved photometric and spectroscopic observations were carried out to conduct period analysis and Doppler tomography mapping.

Results. From radial velocity measurements of the H α line we determined its orbital period to be 0.05592 ± 0.00035 days (80.53min). This period is longer than the first estimate of 76 min by Szkody et al. (2003), but still at the very edge of the period limit for hydrogen-rich CVs. The spectrum shows double-peaked Balmer emission lines flanked by strong broad Balmer absorption, indicating a dominant contribution by the white dwarf primary star, and is similar to the spectra of short-period low-mass transfer WZ Sge-like systems. The photometric light curve shows complex variability. The system undergoes cyclic brightening up to 0.4 mags, which are of semi-periodic nature with periods of the order of 8-12 hours. We also detect a 40.25 min variability of ~ 0.15 mag corresponding to half of the orbital period. Amplitude of the latter increases with the cyclic brightening of the system. We discuss the variable accretion rate and its impact on the hot spot as the most probable reason for both observed processes.

Conclusions. SDSS J123813.73-033933.0 is preliminary classified as a WZ Sge-like short period system with low and unstable accretion rate.

Key words. stars: - cataclysmic variables - dwarf nova, individual: - stars: SDSS J123813.73-033933.0

1. Introduction

Cataclysmic variables (CVs) are close binaries that contain a white dwarf (WD) and a late main-sequence (K-M spectral type) star. The secondary star fills its Roche lobe and transfers mass to the WD through the inner Lagrangian point. More than 1300 CVs are known presently (Downes et al. 2001) and orbital periods have been found for more than 400 systems. The orbital periods range from days to a minimum period of about 70 min for systems with a main-sequence secondary star. An important feature that stands out in the orbital period distribution of CVs is a sharp short-period cut-off at 80min, the 'period minimum' (e.g. Barker & Kolb 2003). Less than a dozen AM CVn-type CVs with even shorter periods are interpreted as CVs with he-

lium star donors. According to the population syntheses, there should be a significant number of systems near the minimum period, which have not been observed (Kolb & Baraffe 1999). Some calculations predict that 99% of the entire CV population should have orbital periods < 2 h (e.g. Howell et al. 1997), but the number of CVs observed above and below the period gap are similar. If the population models are correct, then only a small fraction of the existing CV population has been discovered so far.

About 400 new CVs are expected from the complete realisation of the Sloan Digital Sky Survey (SDSS). The four releases of SDSS have unveiled 132 new CVs (Szkody et al. 2002a, 2003, 2004, 2005). Among them is SDSS J123813.73-033933.0, which was identified as an $r=17.82$ magnitude CV ($u=17.89$, $g=17.78$, $i=17.97$, $z=18.07$) with the extremely short orbital period of 76 min determined from seven spectra obtained by Szkody et al. (2003). The galactic coordinates of the object are $l = 296.51$ and $b = +59.05$, which implies a galactic

Send offprint requests to: S. Zharikov,
e-mail: zhar@astrosen.unam.mx

* Visiting research fellow at Center for Astrophysics and Space Sciences, University of California, San Diego, 9500 Gilman Drive, La Jolla, CA 92093-0424, USA

extinction factor of only $E(B-V)=0.03$ (Schlegel et al. 1998). The proper motion was measured to be $p.m. = 0'.143/\text{year}$ as presented in the USNO B1.0 catalogue (Monet et al. 2003). The optical spectrum of this system shows a blue continuum with broad absorption features around double-peaked Balmer emission lines. The spectral appearance resembles the small, but intriguing, group of so-called WZ Sge objects remarkable for their large amplitude outbursts, long recurrence cycles, and peculiar outburst lightcurves. They are concentrated close to the lower limit of the CV period distribution and are believed to have bounced back from the minimum-period limit; i.e. dwarf novae that have periods that are lengthening after evolving through the period minimum. These are supposed to be those very missing systems with short periods that, according to theoretical calculations, should produce a spike in the number of CVs at the period minimum. However, the discovery and study of them is hindered by their intrinsic faintness, due to the low-mass transfer rates, and infrequent outbursts.

The subject of this paper is a time-resolved simultaneous spectroscopic and photometric study of the CV SDSS J123813.73-033933.0 (hereafter abbreviated as SDSS1238). In Sect.2 we describe our observations and the data reduction. The data analysis and the results are presented in Sect.3 while a discussion and a summary are given in Sects.4 and 5, respectively.

2. Observations

The observations of SDSS1238 were obtained at the Observatorio Astronómico Nacional (OAN SPM¹) in Mexico. Photometric observations were performed on the 1.5m telescope covering a longer time span: 3 nights in April and 4 nights in May 2004. Differential photometry using four field stars as reference was obtained in the V and R broadband Johnson-Cousins filters in long time series with individual exposures ranging from 120 to 180s.

The 2.1m telescope with the B&Ch spectrograph, equipped with a $24\ \mu\text{m}$ (1024×1024) SITe CCD was used for the spectroscopic observations. Spectra were obtained in the first order of 1200 and 400 line/mm gratings. A relatively narrow slit was used (width of $1''.5$) resulting in a spectral resolution of FWHM $2.3\ \text{\AA}$ and $6.2\ \text{\AA}$ for each corresponding grating. Spectroscopic observations were done during four consecutive nights in April and one night in May, 2004 with a total coverage of about 21h with 10 minute individual exposures. The He-Ar lamp was taken every 2-3 hours during the runs for wavelength calibrations, and the standard spectrophotometric stars HZ44, Feige34, Feige67, BD+33 2642 (Oke 1990) were observed (a pair each night) for flux calibrations. At the end, a total of 102 spectra were obtained. The reduction of the images and the extraction of the spectra were done using standard IRAF² rou-

tines commonly used for long-slit spectra. The bias subtraction was applied using overscan strip correction, and spectra were extracted using optimal weights based on the spatial profile. The wavelength calibration was done using multiple arc lamps taken during the night and flux calibration using at least two standard stars observed at different airmasses. During some of these nights we obtained simultaneous photometry of the object in the V band on the accompanying telescope. For those nights we corrected spectra to corresponding photometric fluxes. This, however, does not warrant excellent flux calibration in the blue part of the spectra, since a narrow slit was used with seeing that was usually comparable to the slit width and a permanent E-W orientation of the slit. A log of observations is presented in Table 1.

3. Data analysis.

3.1. Spectrum of SDSS1238

The time-averaged spectrum of SDSS1238 corrected for K1 velocity shifts in the white dwarf frame due to the orbital motion is shown in Fig. 1. The spectrum shows the characteristic features of a short-period, low-mass transfer rate and relatively high inclination cataclysmic variables, like WZ Sge and RZ Leo. The continuum of the SDSS1238 roughly resembles the spectrum of a DA3 type WD. There is no evidence of the presence of the secondary star in the red part of the spectrum, which is also common in this kind of object. There are strong Balmer and weak HeI, HeII emission lines. All emission lines in the spectrum have wide double-peaked profiles, suggesting that they are produced in a high inclination accretion disc and/or the combination of emission lines from the disc and the underlying absorption from the white dwarf primary (see Fig. 1). The symmetric absorption at the wings of emission lines in addition to the central dip indicate a rather stellar origin of the absorption. The double-peaked profile structure of the Balmer lines is preserved during all orbital phases of the system.

The shape of the broad absorption lines agrees with their formation in the high density photosphere of the WD. Similar broad Balmer absorption lines have been detected in a number of other short period dwarf novae (e.g. WZ Sge, GW Lib, BC UMa, or BW Scl). We could not completely rule out a geometrically thin but optically thick disc origin of observed absorptions; however, the hypothetical identification of the observed Balmer absorptions as the photospheric spectrum of the white dwarf has been confirmed by the unambiguous detection of the white dwarf at ultraviolet wavelengths (Gänsicke et al. 2005, Szkody et al. 2002b, Sion et al. 1990) in all above mentioned systems. We determined the WD parameters by fitting Balmer lines of the observed spectrum with a grid of a pure hydrogen model spectra calculated with the NLTE code developed by Werner (1986). The model grid and the fit procedure are described in Napiwotzki (1997). Deviations from LTE are unimportant in the parameter range explored here, but the model atmospheres contain the input physics required for the analysis of DA white dwarfs.

Since the signal-to-noise of our co-added spectrum in the blue/UV part was low, we performed the spectral analysis

¹ <http://www.astrosen.unam.mx>

² IRAF is the Image Reduction and Analysis Facility, a general purpose software system for the reduction and analysis of astronomical data. IRAF is written and supported by the IRAF programming group at the National Optical Astronomy Observatories (NOAO) in Tucson, Arizona. NOAO is operated by the Association of Universities for Research in Astronomy (AURA), Inc., under cooperative agreement with the National Science Foundation

Table 1. Log of observations of SDSS J123813.73-033933.0.

Date (2004y.)	HJD Start+	Telescope	Instrument/Grating	Range/Band	Exp.Time/Num. of Integrations	Duration
Spectroscopy						
14 Apr	109.868	2.1m	B&Ch ¹ 1200l/mm	6000-7100Å	600s×11	1.92h
15 Apr	110.650	2.1m	B&Ch 1200l/mm	6000-7100Å	600s×22	3.84h
16 Apr	111.724	2.1m	B&Ch 400l/mm	4200-7300Å	600s×15	2.93h
17 Apr	112.658	2.1m	B&Ch 400l/mm	5200-8200Å	600s×20	3.27h
17 Apr	112.852	2.1m	B&Ch 400l/mm	3700-6800Å	900s×11	4.65h
19 May	145.710	2.1m	B&Ch 400l/mm	4200-7300Å	600s×23	4.32h
Photometry						
15 Apr	110.737	1.5m	RUCA ²	R	180s×101	5.76h
16 Apr	111.751	1.5m	RUCA	R	180s×119	5.18h
17 Apr	112.653	1.5m	RUCA	V	120s×129	7.22h
16 May	142.675	1.5m	RUCA	V	120s×133	5.38h
17 May	143.663	1.5m	RUCA	V	120s×128	5.51h
18 May	144.646	1.5m	RUCA	V	120s×143	5.80h
19 May	145.652	1.5m	RUCA	V	120s×135	5.64h

¹ B&Ch - Boller & Chivens spectrograph (<http://haro.astrosp.unam.mx/Instruments/bchivens/bchivens.htm>)

² RUCA - CCD photometer (http://haro.astrosp.unam.mx/Instruments/laruca/laruca_intro.htm)

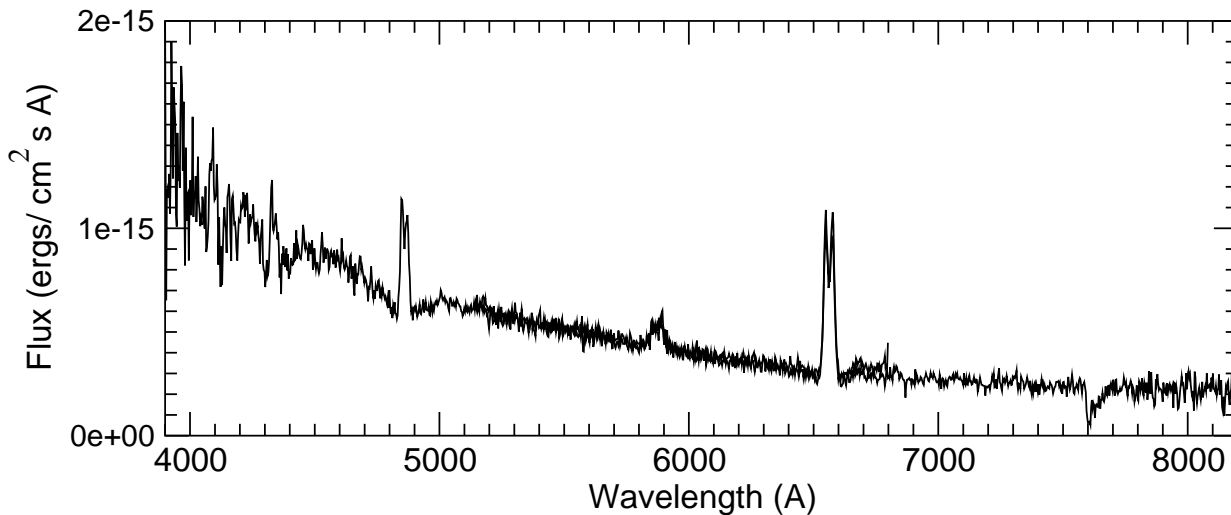


Fig. 1. The low-resolution time-averaged composite spectrum of SDSS1238 (10 spectra 3900 – 6800 Å in blue and 20 spectra 5200 – 8200 Å in red ranges corrected for radial velocity shifts due to orbital motion) is shown.

with the Sloan Survey³ spectrum. The regions contaminated by emission from the disc were excluded from the fit (cf. Fig. 2). Due to the disc contamination it is difficult to determine temperature and gravity simultaneously. Thus we preferred to fix gravity at a range of values (allowed range: $\log g = 7.6\dots 8.2$) and only fit the temperature. The combined best estimate of the WD parameters is $T_{\text{eff}} = 15600 \pm 1000$ K and $\log g = 7.85 \pm 0.25$.

Note that cooler solutions with temperatures below the maximum of the Balmer lines exist as well (T_{eff} in the range 10000 K to 11000 K). The fits are slightly worse, but the differ-

ence in fit quality is not large enough to rule out the cool solutions. Additional information is provided by the photometric colours observed in the course of the Sloan survey: $u - g = 0.06$ and $g - r = -0.05$. The relations of Smith et al. (2002) allow a transformation into Johnson colours: $U - B = -0.79$ and $B - V = 0.15$. Bergeron et al. (1995) computed colours for white dwarfs. A comparison of the observed colours of SDSS1238 with their tabulation yields ≈ 17000 K from the $U - B$ colour and 13000 K from $B - V$. Both results are only consistent with our hot solution. The large difference between the temperatures computed from the two colours are probably explained by the contribution of the disc. The contribution of the Balmer emission lines increases the flux in the g and r filters. For a simple estimate we produced a version of the observed spectrum with the emission lines removed by hand. The spectra were convolved with the transmission curves (Smith et al. 2002) and magnitudes computed for the spectra with and without emis-

³ Funding for the creation and distribution of the SDSS Archive has been provided by the Alfred P. Sloan Foundation, the Participating Institutions, the National Aeronautics and Space Administration, the National Science Foundation, the U.S. Department of Energy, the Japanese Monbukagakusho, and the Max Planck Society. The SDSS Web site is <http://www.sdss.org/>.

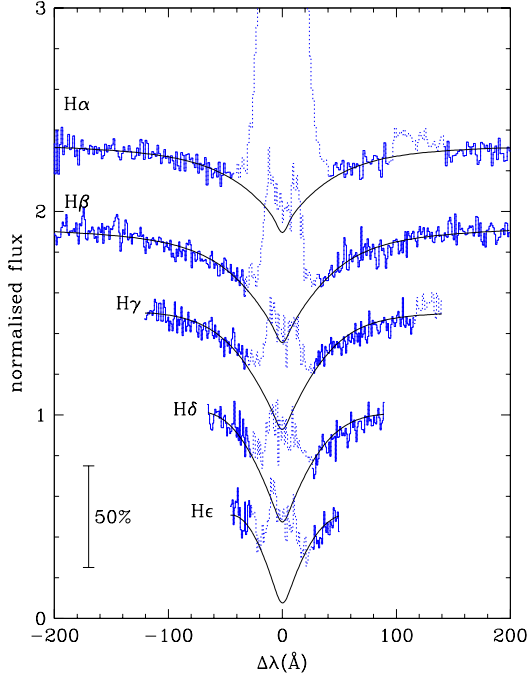


Fig. 2. The WD atmosphere model fitted to the Balmer absorption lines of SDSS1238.

sion lines. The result is that the emission lines increase the flux in g and r by approximately 0.03 mag and 0.06 mag, respectively. This causes a corresponding reddening of the colours of the system as compared to an isolated white dwarf. An additional contribution comes from the continuum of the disc; however, the current observational data does not allow us to perform a quantitative estimate.

3.2. Orbital period determination.

In order to determine the orbital parameters, we measured the radial velocities (RV) from $H\alpha$ and applied the double-Gaussian deconvolution method introduced by Schneider & Young (1980) and further elaborated by Shafter (1983). The optimal value of the separation was determined from the diagnostic diagrams, and the RV values measured for this Gaussian separation were again subjected to a power spectrum analysis in order to refine the period. The photometric and RV data of SDSS1238 were analysed for periodicities using the Discrete Fourier Transform (DFT) code (Deeming 1975) with a CLEAN procedure (Roberts et al. 1987). The $H\alpha$ RV power spectrum is plotted in the left panel of Fig. 3. The maximum peak is at the $17.88218 \text{ day}^{-1}$ frequency, which corresponds to the orbital period of $P_{\text{orb}} = 0.05592 \pm 0.00035$ days. The error of period estimation corresponds to FWHI of the main peak in the power spectrum. One day aliases also come up with lower amplitudes. The derived period is about 4 min longer than the 76 min period recently reported by Szkody et al. (2003) determined from only 7 spectra.

Those RV measurements were fitted with a single sine curve with the orbital period $P_{\text{orb}} = 0.05592$ d:

$$V(t) = \gamma_o + K_1 * \sin(2\pi(t - t_0)/P_{\text{orb}} + \pi),$$

where $\gamma_o = -3 \pm 2 \text{ km/s}$ is the systemic velocity, and $K_1 = 80 \pm 4 \text{ km/s}$ the semi-amplitude of the $H\alpha$ radial velocity. The time of observation is t , and epoch $t_0 = 2453112.687 \pm 0.001$ HJD corresponds to the +/- zero crossing of the radial velocity curve. Fig. 3, right, shows the radial velocity data of $H\alpha$ emission line folded with the spectroscopic orbital period (0.05592 days) and its best sinusoidal fit. The central absorption in $H\alpha$ shows the same RV as the emission line (see Fig. 6, left).

3.3. Photometric light curves

We obtained quite unusual results from the analysis of the photometric data presented in Fig. 4. SDSS1238 shows two types of variabilities:

- a *long-term variability* (in the range of 8-12h) with $\sim 0.45 \text{ mag}$ amplitude;
- a *short-term variability* with half the orbital period ($\sim 40.3 \text{ min}$), which is more evident in the bright part of the long-term variability, reaching $\sim 0.35 \text{ mag}$.

No eclipses are detected in the light curves of the system.

The left panel of Fig. 5 shows the power spectrum computed for selected (bright) parts of the light curve (data marked by open circles in the Fig. 4). Two practically equal peaks can be seen, one at a frequency that corresponds to $2/P_{\text{orb}} = 35.76 \text{ day}^{-1}$ and the other at 36.76 day^{-1} , being a 1-day alias. The main peak corresponds to half ($P_{\text{orb}}/2 = P_{\text{phot}}^{\text{short}} = 40.3 \text{ min}$) of the orbital period. The selected photometric data points folded with the photometric period $P_{\text{phot}}^{\text{short}}$ are shown in the right panel of Fig. 5. The short-term photometric variability is sinusoidal (Fig. 5, right) although the amplitude varies. Portions of the light curve of SDSS1238, together with simultaneous $H\alpha$ emission and absorption RV measurements and their corresponding fits, are plotted all together in Fig 6. The short-term, half orbital period variability appears to be coherent and stable with highly variable amplitude. The amplitude of short-term variability correlates with the cyclical brightness variations described here as long-term variability. The maximums of the half-orbital period photometric variability occur at the $\phi = 0.375$ and 0.875 of orbital phases of the system as demonstrated in the right panel of Fig. 5 and in Fig. 6. We did not find any phase shifts from one observational run to another (within 2 months).

The long-term variability (LTV) was instantly detected during the first observations in April 2004 (Table 1). The brightness of the object changes up to 0.4 magnitudes (Fig. 4). The period analysis of the photometric data obtained during the three first nights revealed a certain periodicity of these changes. In the May observations we confirmed the existence of this long-term variability; however, the data from the first two nights in May were either out of phase or the periodicity of LTV was not strict. The final two nights of the May observations showed good coherence with the April data. The amplitude of LTV in the May observations remained the same as in April. The long-term variability was also detected by Woudt & Warner (2004) during several sets of observations in the beginning of 2004. Woudt & Warner (2004) did not find any exact period of LTV either. The power spectrum from the complete data sample is confusing and difficult to interpret. For natural

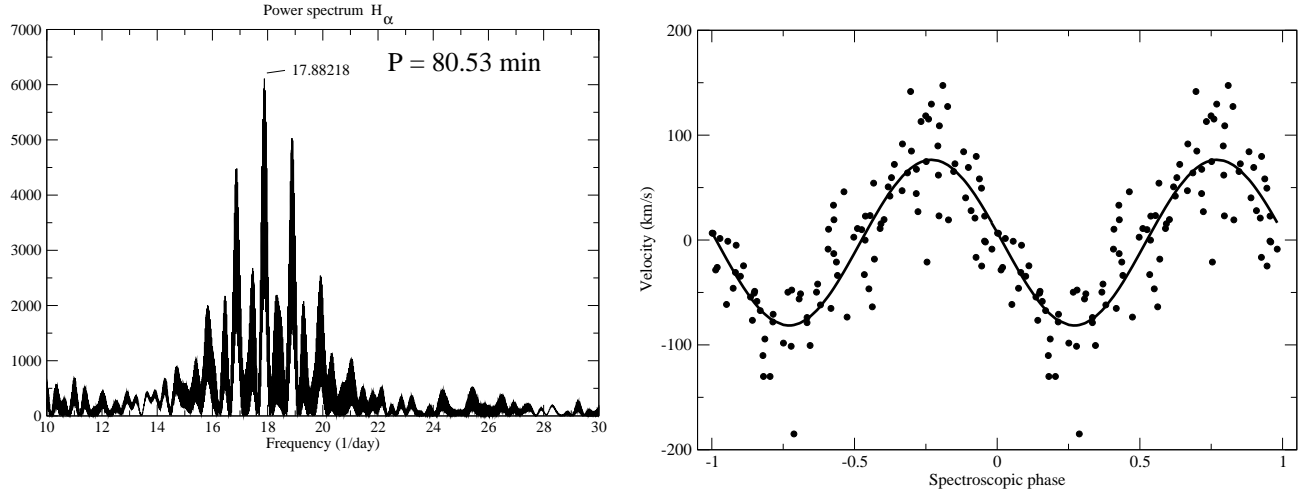


Fig. 3. Left) The power spectrum of the H α radial velocity curve. The maximum peak in frequency corresponds to the orbital period of the system $P_{\text{orb}}=0.05592$ day. Right) The radial velocity measurements of the H α emission line folded with the spectroscopic orbital period (0.05592 days) and its best fit sinusoid.

reasons observational runs are shorter than any plausible period of LTV, and the amount of observational data is not enough for any firm conclusion about the existence of a strict and coherent period. At the mean time it is clear that LTV has a cyclical, quasi-periodic nature at least on short time scales of days about 8-12 hours). These cycles are much shorter than the shortest known dwarf nova outburst cycles and neither the profile of the light curve nor the amplitude are similar to the outbursts.

Amazingly, the amplitude of the short-term variability correlates with this semi-periodic LTV, and its amplitude increases from less than ~ 0.1 mag in the faint part of the light curve to up to ~ 0.35 mag in the bright part of the LTV curve.

3.4. Tomography

The H α Doppler maps⁴ were constructed separately for the faint (Fig. 7, top panels) and bright (Fig. 7, bottom panels) parts of “LTV-period” (see Fig. 6). 28 spectra obtained on April 17 (JD 112) and 15 spectra obtained on May 19th (JD 145) were used for the faint (20 spectra) and the bright parts (23 spectra) of the “LTV-period”. The system parameters used for Doppler tomogram mapping are shown on the top of Doppler maps in Fig. 7. We used the average mass $\bar{M}_{wd} = 0.69M_{\odot}$ for WDs residing in CV below the period gap (Smith & Dhillon 1998). That leads to the mass ratio $q = M_2/M_1 < 0.18$ obtained using the Howell et al. (2001) relationship for secondaries in CVs. The inclination angle is also chosen arbitrarily, as a compromise for high K_{em} system in the absence of eclipses.

The Doppler tomograms show different states of accretion in the system. In the low state the two bright symmetric arch-shaped regions at velocity coordinates (-200km/s, -800km/s) and (600 km/s, 450km/s) in Fig. 7, (right, top) look like the

spiral wave structures in the Doppler maps of IP Peg and EX Dra (Harlaftis et al. 1999, Joergens et al. 2000). In the bright state (Fig. 6 and 7, right, bottom), we get only one bright spot (-600 km/s, 500 km/s) at the expected place where the mass transfer stream hits the accretion disc. This spot moves out from the stream path if we significantly increase mass of the primary WD, thus proving that the system parameters are within reasonable values. The spot is completely absent in the low state (Fig. 7, right, top). This difference of the Doppler tomograms built with the distinct spectra from the faint and bright parts of the light curve probably testifies to a rapid (~ 8 -12h) change in \dot{M} and the accretion disc structure from one to another phase of LTV.

It should be noted that the number of spectra, the phase resolution (exposure time/orbital period = 0.12), and S/N ratio of spectra are not high enough to construct reliable Doppler tomograms. We cannot be confident of detecting spiral arms, as they might be artifacts arising from data quality and contrast of the picture, although brightening of the hot spot in the bright phase of LTV is less doubtful. It appears in the right place and shape and replicates itself in the H β line (not shown here).

4. Discussion

SDSS1238 is a remarkable CV on the lower edge of the CV period distribution, which exhibits a number of interesting features that define the small class of CVs known as WZ Sge stars. In addition to these features, it undergoes frequent and cyclical brightness changes, defined here as LTV, that sets it apart from other similar CVs or any other CV as a matter of fact.

The observed period minimum for CVs with hydrogen-rich secondaries is about 77min (Kolb & Baraffe 1999). According to our current understanding the number of CVs should peak close to the 80 min period limit, as they evolve to the boundary where they bounce back (see Patterson 1998 and references therein). If this is true then only a tiny part of that presumed stockpile is recovered. There are only about 50 systems

⁴ For details of the Doppler tomography method and interpretation see Marsh & Horne (1988), Marsh (2001). We have generated SDSS1238 Doppler maps by using Spruit’s code (Spruit, 1998 Maximum entropy method): <http://www.mpa-garching.mpg.de/~henk/pub/dopmap/>.

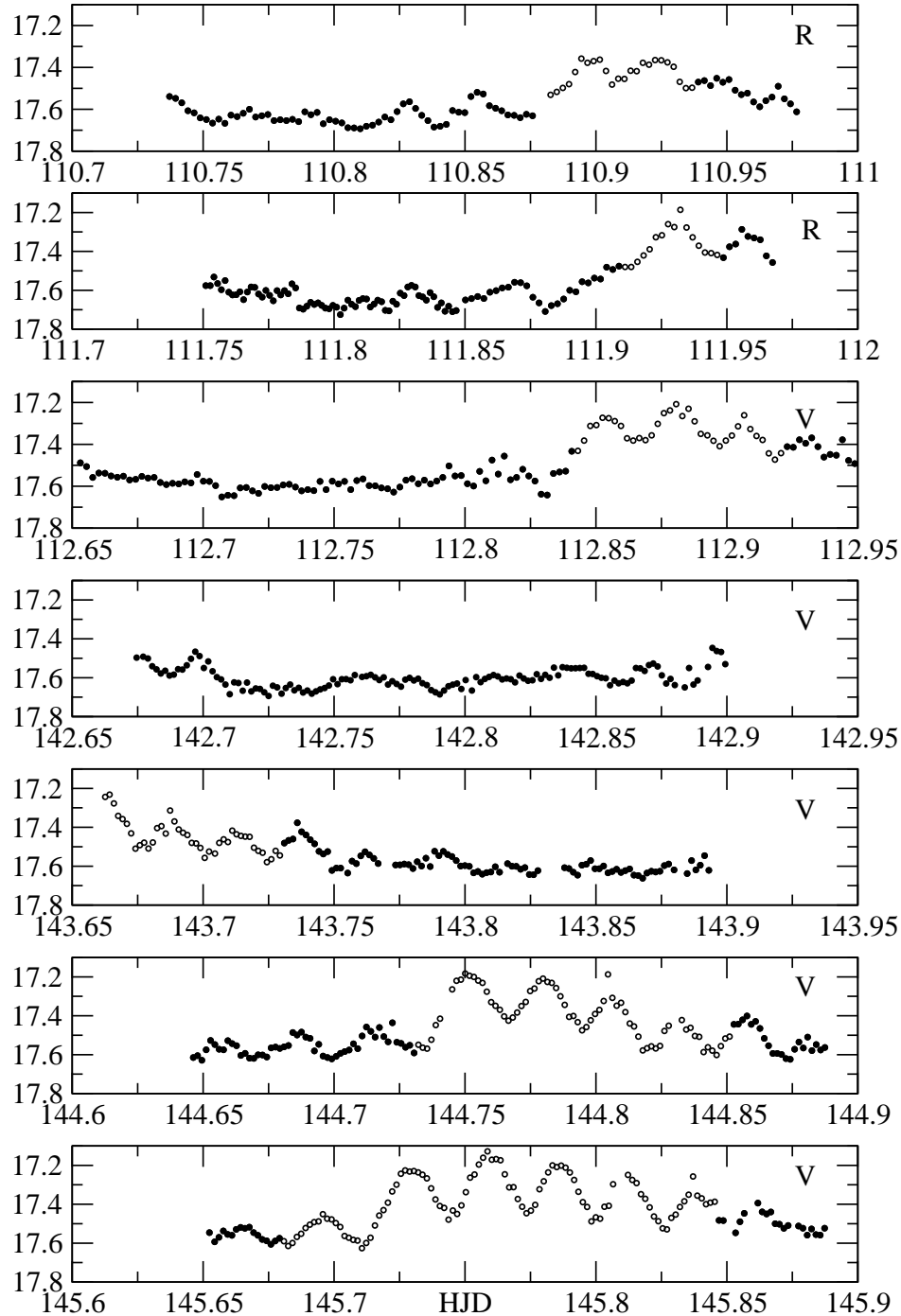


Fig. 4. The light curves of SDSS1238 in *V* and *R* bands. The reference for magnitude is the USNO B1 value of SDSS1238 $r=17.6$ arbitrarily assigned to the minimum of the measured magnitudes. Each night is presented in a separate panel. The open circles mark the data used for the period search of short-term variability (see text).

known above the period minimum to up to ~ 90 min. Part of the sample in this period range are SU Uma (together with ER Uma) objects (about 20 of them), some are magnetic CVs (10 AM Her and 6 DQ Her objects) and few are firmly classified as WZ Sge stars based on infrequent outbursts with distinct high amplitude and echo re-brightening during fading from the outburst (Patterson et al. 2002). The WZ Sge objects are probably the only ones identified as evolved/bounced systems.

Several other stars are proposed as candidates to the WZ Sge class based on their quiescence properties. SDSS1238 bears certain resemblance to WZ Sge stars, particularly because of absorption features in the spectrum and the double humped light curve. Besides these observational characteristics, the relatively low temperature deduced for the white dwarf (see Urban et al. 2000) indicate that SDSS1238 may belong to this enigmatic group of objects.

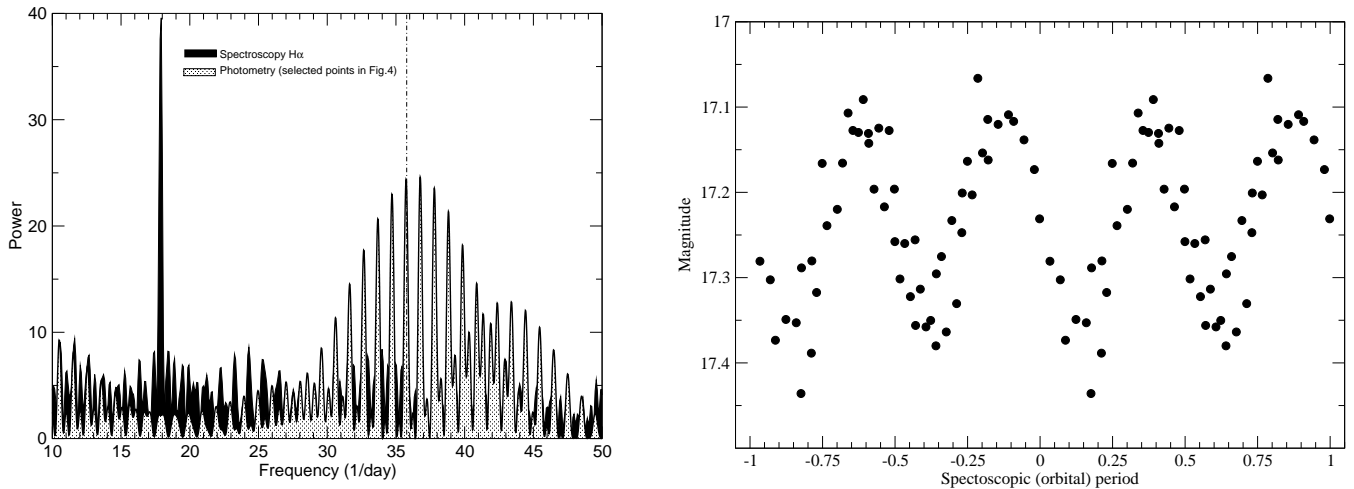


Fig. 5. Left) The CLEANed power spectrum of $H\alpha$ RVs and power spectrum of selected photometry points from the bright part of the light curve (see Fig. 4). The photometric period is 2 times shorter than the orbital period. Right) The light curve comprised of the selected points (19 May, HJD between 2453145.75 and 2453145.84 with long-term variability trend removed) folded with the short-term variability period. The maximum semi-amplitude of the variability is about 0.2 mag.

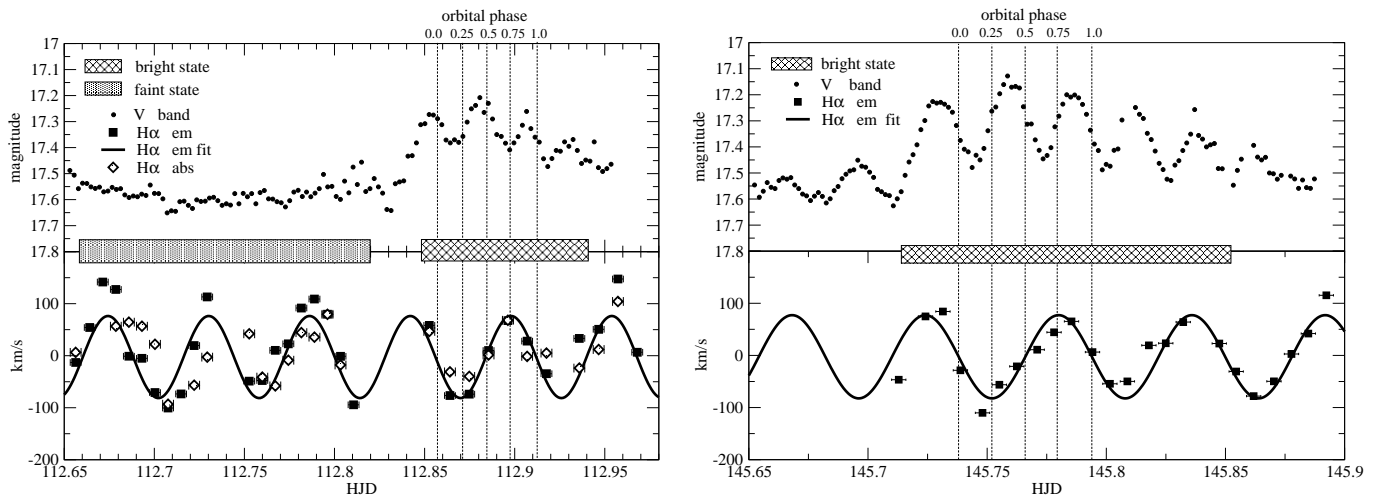


Fig. 6. The light curves (top panels) and RV of $H\alpha$ with corresponding best fit curves (low panels) of SDSS1238 for 17 April (right) and 19 May (left). The full squares (low panels) and open diamonds (low right panel) present the $H\alpha$ emission and absorption (central) components, respectively. Vertical dashed lines show selected orbital phases of the system. Two shaded bands mark portions of data in the bright and faint states of the SDSS1238 light curves used for Doppler tomography analysis.

While the reason for the double-humped light curve is not understood well in these systems, it appears to be more or less widespread among certain short-period CVs. True, in the majority of them it appears only during the outburst. In short period CVs, the extremely late type secondary star is so dim that it usually passed undetected whether spectroscopically or photometrically. If SDSS013701.6-091234.9 may be anomalous in that sense (Szkody et al. 2003, Pretorius et al. 2004), in SDSS1238 the secondary is not detected spectroscopically and the double hump light curve (detected in V band with the same amplitude as in the R) can by no means be caused by the ellipsoidal shape of the secondary. As already mentioned, in the majority of other systems the double-humped light curve is observed during outbursts. According to Patterson et al. (2002) the double-hump wave appears in WZ Sge within 1 day of

outburst maximum and is then replaced by a common super-hump that develops in a normal manner. The physical processes producing double humps in outbursts are not clear either. In Patterson et al. (2002) there is a discussion of possible causes and references to the proposed models without firm conclusions. Authors favour the model in which the development of a strong two spiral-arm structure at the beginning of an outburst, when the 2 : 1 eccentric resonance is reached, produces the desired waveform in the lightcurve (Osaki & Meyer 2002). Within the evidence supporting this model is the detection of a two-armed spiral in the Doppler tomograms of WZ Sge during the first few days of outburst (Steehs et al. 2001; Baba et al. 2002). Another possible explanation of the double-humped light curve (Patterson et al. 2002) is a sudden increase in transferred matter that creates a hot spot at the disc's outer edge.

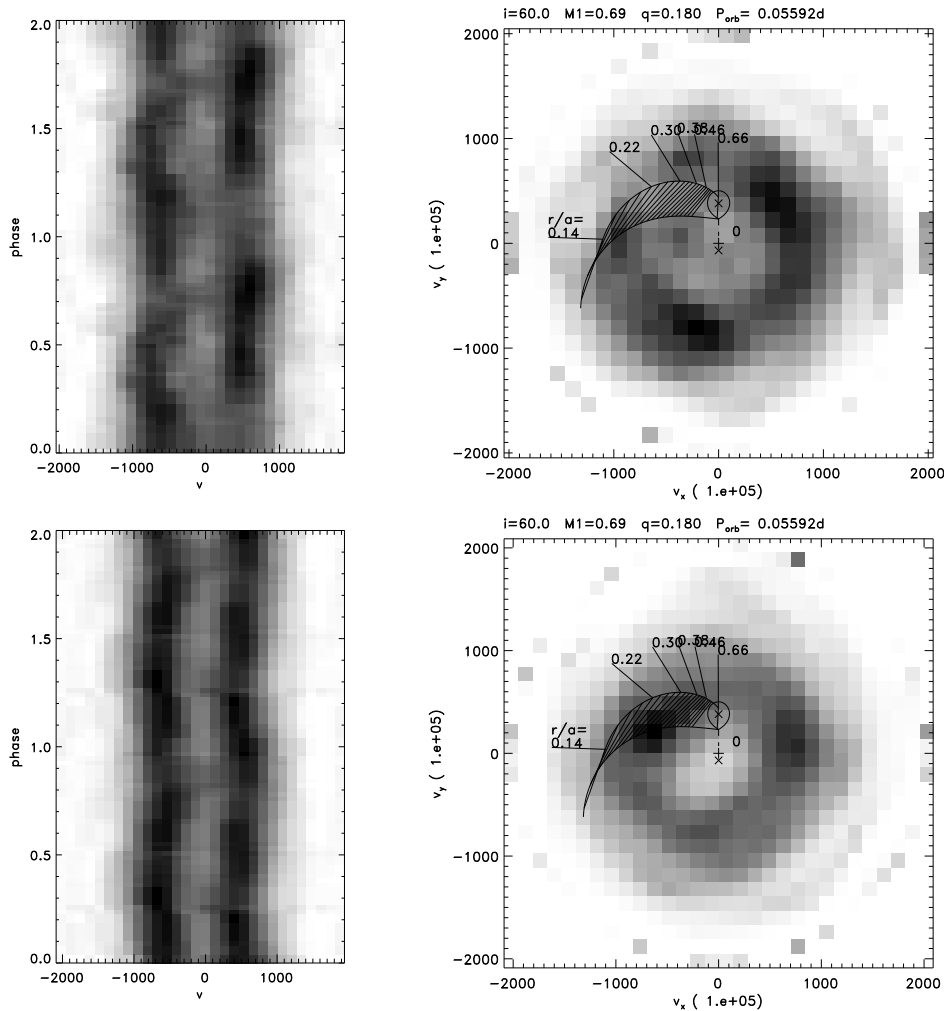


Fig. 7. The $H\alpha^{\text{faint}}$, $H\alpha^{\text{bright}}$ trailed spectra folded with the orbital period of the system and their correspondent $H\alpha$ Doppler maps (right panels) constructed for the faint (top) and bright (bottom) portions of the long-term variability (see Fig. 6). Adopted parameters of the system are shown at the top of the Doppler maps.

A hot spot is a common feature in CVs and in many high inclination systems it produces a distinctive shoulder in the light curve. The maximum in the optical light curve originating in such a hot spot is around $\phi = 0.85$, when the disc is seen face on. The weaker maximum at opposite $\phi \sim 0.3$ may be naturally explained by viewing the hot spot, partially obstructed by the accretion disc, from the opposite side (Silber et al. 1994). If we assume that in low \dot{M} systems in quiescence the disc is optically thin and tiny, then the hot spot can be visible through it and create the possibility of a double-humped light curve with maxima at phases $\phi \sim 0.3$ and $\phi \sim 0.8$.

Incidentally we detect both phenomena: (i) an unhomogeneous spiral-arm-like structure is detected at the bottom of LTV, and (ii) the accretion stream/disc impact hot spot dominating Doppler tomogram during the bright part of LTV. As in the case of WZ Sge (Lasota et al. 1995; Hameury et al. 1997), the hot spot model suggests a sudden burst of mass transfer. The authors argue that the irradiation of the secondary provides the basis for the mass transfer rate change. Of course both models were developed to explain the observed features

of WZ Sge and similar in outbursts. However the phenomenon of double humps was observed in several occasions in the quiescent state in WZ Sge and AL Com (Patterson et al. 1996) and a few other short period WZ Sge-like systems IY UMa (Rolfe et al. 2005), WX Cet (Rogoziński & Schwarzenberg-Czerny 2001), SDSS013701.06-091234.9 (Szkody et al. 2003, Pretorius et al. 2004), BW Scl/RX J2353.0-3852 (Augusteijn & Wisotzki 1997; Abbott et al. 1997). In quiescence there is no chance that the disc extends as far as the 2:1 resonance radius, hence the bright spot is a better explanation for the double humps. Besides, in most of the other systems, the second hump is often smaller in amplitude. This is good evidence of a bright spot that is weakened as it is observed on the far side of the disc and through it. It is convincingly demonstrated by Rolfe et al. (2005) using high S/N spectra and Doppler tomography that the double hump lightcurve originates from the hot spot.

Our data on SDSS1238 were obtained certainly outside of the outburst regime. Therefore we simply assume, by analogy with other similar systems, that the double-humped light curve profile is a result of increasing hot spot brightness during the

bright phase of LTV. Then, naturally, the increased brightness of the spot and the system as a whole can only be explained in terms of increased \dot{M} . Why the mass transfer rate and hence the brightness vary quasi-periodically on such short time scales (7-12 hours) is a separate and very interesting question. One possible explanation is the irradiation of the secondary as favoured by Hameury et al. (1997). Although this idea was originally suggested to explain the triggering of the superoutburst in the WZ Sge systems, it is quite possible that the very late type secondary in SDSS1238 barely fills its Roche lobe and maintains a delicate balance. Then, the slightest irradiation from the bright, hot spot will expand the secondary to fill its Roche lobe thereby expelling increased amounts of matter toward the primary. The secondary will then shrink, decreasing the mass transfer only to be irradiated again and to undergo another cycle once the matter reaches the edge of accretion disc and re-brightens it.

In no other system than SDSS1238 is cyclical brightening or LTV detected. According to our proposed scenario this can be due to the particular mass ratio established in SDSS1238. For example, in WZ Sge the estimated WD mass is substantially higher, which will lead to a much smaller secondary Roche lobe.

5. Summary

The principal results can be summarised as follows:

1) The spectrum of the system shows double-peaked Balmer emission lines from the disc and broad Balmer absorption lines originating in the photosphere of the white dwarf. The WD surface temperature of 15600 K obtained from the model fit to the spectrum is within the WD temperature range (15 000 -22 000K) observed in the short period systems below the period gap (see Urban et al. 2000)

2) The spectroscopic orbital period of the SDSS1238 is $0.05592 \text{ day} \pm 0.00035$.

3) The system shows two types of photometric variabilities:

- a *long-term variability (LTV)* with amplitude ≈ 0.45 mag and roughly 8-12 hours quasi-period;

- a *short-term variability* with amplitude about ≈ 0.35 mag in the bright part of LTV with a period two times shorter than the orbital period of the system.

4) The analysis of Doppler maps constructed for the bright and faint parts of LTV shows that the change of mass transfer in the system is the most probable cause of the long-term variability and that the hot spot dominates the radiation from the accretion disc at the top of the LTV.

5) The hot spot is also the probable source of the double humped light curve. The brightness, as well as amplitude of the humps, varies in a cyclical manner and is certainly a result of the variable mass transfer rate.

6) The cause of quasi-periodic flux variability (LTV) and hence of the variable rate of mass transfer is not clear, but could be the result of the irradiation of the secondary.

Acknowledgements. This work was supported in part by DGAPA project IN-110002. GT acknowledges the support of a UC-Mexico

fellowship. R.N. acknowledges the support by a PPARC Advanced Fellowship. VN acknowledges support of IRCSET under their basic research program and the support of the HEA-funded CosmoGrid project. We thank anonymous referee, for his comments that lead to an improved presentation of the paper.

References

- Abbott, T. M. C., Fleming, T. A., Pasquini, L. 1997, A&A, 318, 134
 Augustejn, T., Wisotzki, L. 1997, A&A, 324L, 57
 Baba, H., Sadakane, K., Norimoto, Y., et al. 2002, PASJ, 54L, 7
 Barker, J., Kolb, U. 2003, MNRAS, 340, 623
 Bergeron, P., Wesemael, F., Beauchamp, A. 1995, PASP, 107, 1047
 Beuermann, K., Baraffe, I., Kolb, U., Weichhold, M. 1998, A&AS, 337, 403
 Deeming, T. J. 1975, Ap&SS, 36, 137
 Downes, R. A., Webbink, R. F., Shara, M. M., et al. 2001, PASP, 113, 764
 Gänsicke, B. T., Szkody, P., Howell, S. B., & Sion, E. M. 2005, ApJ, 629, 451
 Joergens, V., Spruit, H. C., Rutten, R. G. M. 2000, A&A, 356L, 33
 Hameury, J.-M., Lasota, J.-P., Hure, J.-M. 1997, MNRAS, 297, 937
 Harlaftis, E. T., Steeghs, D., Horne, K., et al. 1999, MNRAS, 306, 348
 Howell, S. B., Rappaport, S., Politano, M. 1997, MNRAS, 287, 929
 Howell, S.B., Nelson, L., Rappaport, S. 2001, ApJ, 550, 897
 Kolb, U., Baraffe, I. 1999, MNRAS 309, 1034
 Lasota, J. P., Hameury, J. M. Hure, J. M. 1995, A&A, 302L, 29
 Marsh, T. R., Horne, K. 1988, MNRAS, 235, 269
 Marsh, T. R. 2001, "Doppler Tomography", Astrotomography, Indirect Imaging Methods in Observational Astronomy, Edited by H.M.J. Boffin, D. Steeghs and J. Cuypers, Lecture Notes in Physics, vol. 573, p.1
 Monet, D., Levine, S. E., Canzian, B., et al. 2003, AJ, 125, 984
 Napiwotzki, R. 1997, A&A, 322, 256
 Oke, J. B. 1990, AJ, 99, 1621
 Osaki, Y., Meyer, F. 2002, A&A, 383, 574
 Panei, J. A., Althaus, L. G., Benvenuto, O. G. 2000, A&A, 353, 970
 Patterson, J., Augustejn, T., Harvey, D. et al. 1996, PASP, 108, 748
 Patterson, J. 1998, PASP, 110, 1132
 Patterson, J., Masi, G., Richmond, M. W., et al. 2002, PASP, 114, 721
 Pretorius, M. L., Woudt, P. A., Warner, B., et al. 2004, MNRAS, 352, 1056
 Roberts, D. H., Lehar, J., Dreher, J. W. 1987, AJ, 93, 968
 Rogoziecki, P., Schwarzenberg-Czerny, A. 2001, MNRAS, 323, 850
 Rolfe, D. J., Haswell, C. A., Abbott, T. M. C., et al. 2005, MNRAS, 357, 69
 Schneider, P. B., Young, P. 1980 ApJ, 238, 946
 Schlegel, D., Finkbeiner, D., Davis, M. 1998, ApJ, 500, 525
 Silber, A. D., Remillard, R. A., Horne, K., Bradt, H. V. 1994, ApJ, 424, 955
 Sion, E. M., Leckenby, H. J., & Szkody, P. 1990, ApJ, 364, L41
 Shafter, A. W. 1983, ApJ, 267, 222
 Smith, D. A., Dhillon, V. S. 1998, MNRAS, 301, 767
 Smith, J. A., Tucker, D. L., Kent, S., et al. 2002, AJ, 123, 2121
 Spruit, H. 1998, astro-ph/9806141
 Steeghs, D., Marsh, T., Knigge, C., et al. 2001, ApJL, 562, 145
 Szkody, P., Anderson, S. F., Agüeros, M., et al. 2002a, AJ, 123, 430
 Szkody, P., Gänsicke, B. T., Sion, E. M., & Howell, S. B. 2002b, ApJ, 574, 950
 Szkody, P., Fraser, O., Silvestri N., et al. 2003, AJ, 126, 1499
 Szkody, P., Henden, A., Fraser, O., et al. 2004, AJ, 128, 1882
 Szkody, P., Henden, A., Fraser, O., et al. 2005, AJ, 129, 2386
 Urban J., Lions K., Mittal R., et al. 2000, PASP, 112, 1611
 Werner, K. 1986, A&A, 161, 177
 Woudt, P., Warner, B. 2004, private communication.

List of Objects

'SDSS J123813.73-033933.0' on page 1
'SDSS J123813.73-033933.0' on page 1
'SDSS J123813.73-033933.0' on page 1
'WZ Sge' on page 2
'SDSS J123813.73-033933.0' on page 2
'SDSS1238' on page 2
'HZ44' on page 2
'Feige34' on page 2
'Feige67' on page 2
'BD+33 2642' on page 2
'SDSS1238' on page 2
'WZ Sge' on page 2
'RZ Leo' on page 2
'SDSS1238' on page 2
'SDSS1238' on page 3
'SDSS1238' on page 4
'SDSS1238' on page 5
'SU Uma' on page 6
'ER Uma' on page 6
'AM Her' on page 6
'DQ Her' on page 6
'WZ Sge' on page 6
'WZ Sge' on page 6
'SDSS1238' on page 6
'SDSS1238' on page 7
'SDSS1238' on page 7
'WZ Sge' on page 7
'WZ Sge' on page 8
'WZ Sge' on page 8
'SDSS013701.06-091234.9' on page 8
'BW Scl/RX J2353.0-3852' on page 8
'SDSS1238' on page 8
'WZ Sge' on page 9
'SDSS1238' on page 9
'SDSS1238' on page 9
'SDSS1238' on page 9
'WZ Sge' on page 9
'SDSS1238' on page 9